SAND2016-10049R

Microstructural evolution of thin polycrystalline metallic films under extreme conditions

Fadi Abdeljawad
Sandia National Laboratories
Albuquerque, NM 87185

Abstract

Thin films are materials systems that are widely used in applications ranging from electronics and optical devices to industrial and biomedical ones. However, these systems are unstable against various homogenization processes and aging mechanisms (grain growth, coarsening, surface evolution, and diffusion of species) even at low service temperatures. In this work, we examine the role of various aspects of microstructure (grain boundary types and characters, free surfaces, surface diffusion, and thermal grooves) on the thermal aging of such systems. Existing experimental tools will be leveraged to characterize thin films, i.e., in-situ quantitative thermal annealing, and provide direct comparisons to predications emerging from a recently developed meso-scale model via Precession Electron Diffraction (PED). Parametric studies will be conducted to gain insights on the role of each of the aforementioned aspects of microstructure on the dynamics. Herein, we will focus on "hard" gold thin films (with alloying elements like Co, Ni, or Fe) as they are materials of choice in a wide range of applications at Sandia. Initially, pure gold systems are examined and future studies will focus on microstructure evolution in the presence of alloying elements and second-phase particles.

Introduction

Films and thin layers of metallic materials are ubiquitous in electronic devices, for example as conductive paths in circuits and electrical contacts. As a result of vapor or solution deposition processing techniques, these materials often exhibit ultra-fine grain (grain size <1 μm) or nanocrystalline (grain size <100 nm) microstructures. Structural stability is of chief interest, as the high boundary density both heavily influences material properties and can contribute to rapid coarsening, or thermal aging, at moderately elevated temperatures, or even at ambient conditions over time. A predictive understanding of the microstructural evolution processes requires considerable knowledge of both the behavior of individual grain boundaries and the influence of nearby surfaces.

The velocity of a grain boundary can be expressed in terms of its mobility and a thermodynamic driving force, the latter of which can be expressed in terms of the energy and curvature of the boundary. It has long been known that grain boundary energy depends on the structure of the boundary [1]. Similar dependencies have been shown for grain boundary mobility [2]. In real materials, however, the actual motion can be affected by additional factors, such as pinning by various obstacles. For grain boundaries that intersect a free surface, grooves are expected to inhibit grain boundary motion [3]. In the case of thin films, it has been hypothesized that groove drag should come to dominate grain boundary motion. A full characterization of grain boundary motion in such a system requires knowledge of the structures of both the grain boundaries and surface grooves.

In this work the same set of grain boundaries in nanocrystalline Au thin films (nominally 40 nm) were characterized after annealing to increasingly elevated temperatures. This accelerated anneal protocol mimics thermal aging of thin films under extended time scales. Precession electron diffraction (PED) orientation mapping [4] provided axis-angle descriptions of individual grain boundary misorientations, while atomic force microscopy (AFM) revealed the surface structure and groove depths. These datasets were directly incorporated into a phase field model with tunable parameters for anisotropic grain boundary energies and mobilities, surface diffusion, as well as drag induced by grain boundary grooves.

Methods

Au films nominally 40 nm in thickness were deposited onto NaCl single crystals by magnetron sputtering. Prior to the deposition, the NaCl substrates were UV/ozone cleaned and baked at 65 °C for 1 h. The base pressure prior to deposition was approximately 5×10^{-7} torr. After the deposition, the substrates were cleaved into pieces approximately 1 mm × 1 mm, and the resulting film pieces were floated in a mixture of deionized water and isopropanol. The film pieces were collected on 400 mesh Au or Mo TEM grids. Atomic force microscopy was performed in peak force tapping quantum nanoscale mechanical (QNM) characterization mode over areas of 2 µm × 2 µm and 500 nm × 500 nm. A cantilever with 8 nm nominal tip radius was utilized, with scan rate of 0.1 Hz and 1 nN amplitude setpoint.

The samples were loaded in a TEM heating holder (Hummingbird Scientific, Lacey, WA, USA). Precession electron diffraction (PED) orientation mapping was performed in an area near the AFM scan with a probe diameter of approximately 8 nm and precession angle of 0.3°. A grid of 425 × 425 points was collected at 4 nm $step^{-1}$ resulting in a mapped area of 1.7 µm × 1.7 µm. It was found that 7 precessions $step^{-1}$ (0.07 s $step^{-1}$) resulted in an acceptable balance between diffraction pattern quality and total acquisition time (approximately 3.5 h). Annealing experiments were performed in a JEOL 2100 HT TEM [5]. The samples were first brought to a temperature of 200 °C at a heating rate of 5 °C min^{-1}, and then held for 1 h. The temperature was then ramped again to 275 °C and held for an additional 1 h. Video was collected at 5 frames s^{-1} during the temperature ramps and holds. The holder was then allowed to cool to ambient temperature in order to minimize thermal drift. Once cooled, the PED orientation mapping was repeated. Finally, AFM characterization was performed a second time, with parameters similar to the initial measurements.

An additional experiment was performed in which a second sample was similarly ramped at 5 °C min^{-1} to 125 °C, held at temperature for 1 h, cooled, and characterized by PED mapping. This procedure was repeated for temperatures of 225 and 325 °C, resulting in three snapshots of the same area of the sample after exposure to these successively higher temperatures.

Results and Discussion

In the as-deposited state, the first sample was found to have a nanocrystalline structure, as expected. The initial AFM scans in Figure 1a and c revealed surface features, but none that were readily identifiable as grains. In contrast, after annealing plate-like protrusions were clearly identifiable, as shown in Figure 1b and d. Note that these scans are from the same general area, but not necessarily the same grains.

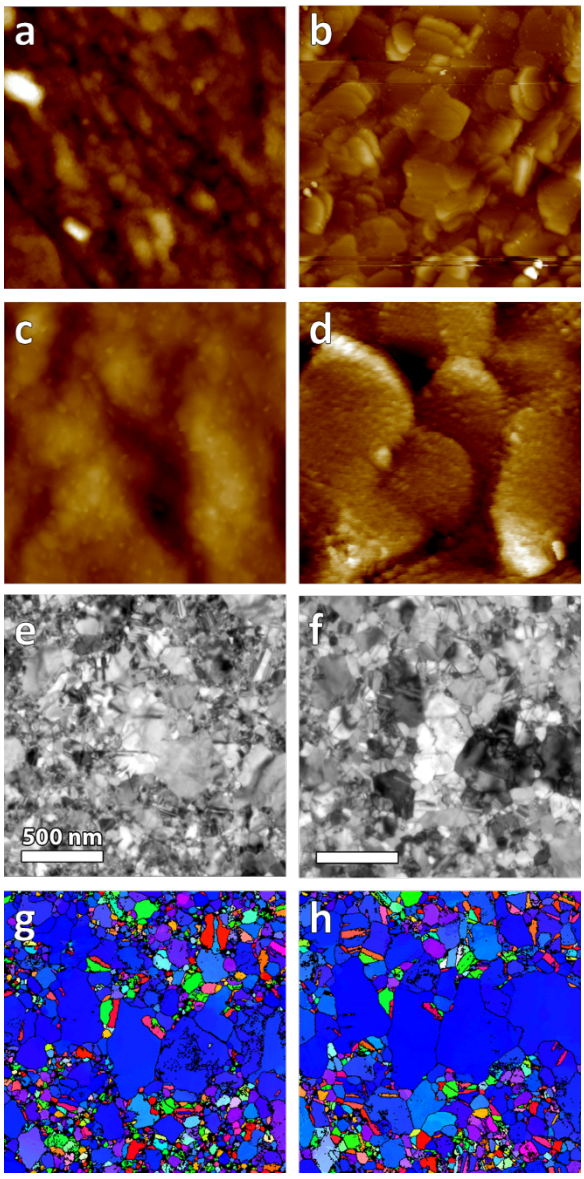

Figure 1: Images from multi-analyses of the Au film before and after *in situ* annealing in the TEM. (a-d) AFM, (e,f) TEM, (g,h) PED orientation mapping. The AFM images show representative images taken from a similar general area, while the TEM and PED images show the same grains before and after the annealing experiment. Orientations represented in (g) and (h) are shown with respect to the page normal. Grain boundaries (>3° misorientation criterion) are drawn in black.

The same area of interest was successfully tracked throughout the annealing process in the TEM. The earliest instances of grain growth were observed around 100 °C. Annealing of the first sample was stopped after the 1 h hold at 275 °C, as shrinking and tearing of the film threatened to destroy the area of interest.

In the TEM micrograph and PED map collected before (Figure 1 e-f), several large grains were clearly apparent in the center. The larger grains were mostly (111) oriented, although other orientations were

apparent. In contrast, the smaller surrounding grains showed an assortment of orientations. Boundaries among the larger grains were readily identifiable for the most part. However, the small surrounding grains were not so clearly defined. After annealing grain growth and boundary movement were apparent in both small and large grains, as is apparent in Figure 1 (g-h). Among large grains, some boundary movement was observed, however, the most dramatic changes were the elimination of many of the smaller grains. However, it was difficult to identify the specific details of many of these boundaries, as many of these especially fine-grained areas did not index well due to multiple grains overlapping through the thickness of the film.

In an effort to track more easily identifiable boundaries throughout the annealing process, a second sample was subjected to a similar temperature ramp and hold process at 125 °C. This low-temperature anneal served to coarsen the smaller grains in order to achieve a clearer starting structure.

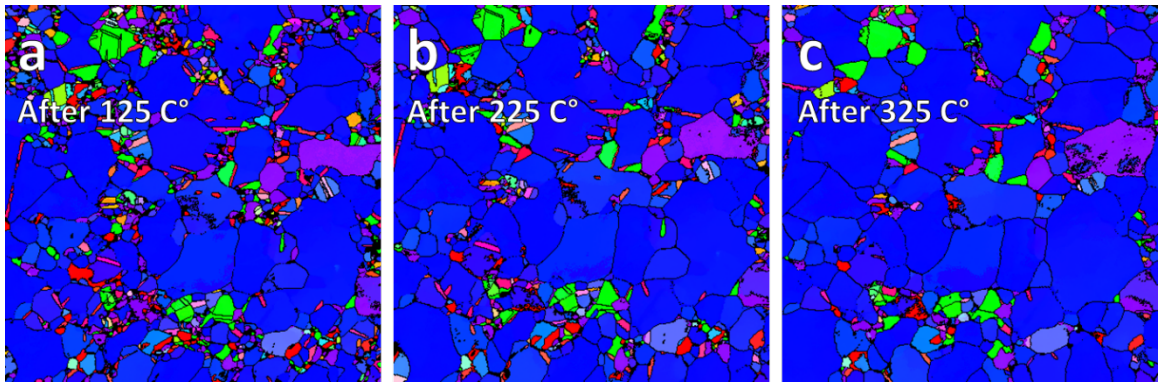

Figure 2: PED orientation maps from the second sample after annealing to (a) 125 °C, (b) 225 °C, and (c) 325 °C. Grain boundaries (>3° misorientation criterion) are drawn in black.

The results from the second annealing experiment are illustrated in Figure 2. It is clear that the 125 °C initial anneal drove recrystallization in the smallest grain, leading to a greater number of identifiable grain boundaries.

To demonstrate the role of both grain boundaries and free surfaces on the microstructure evolution, we developed a meso-scale phase field model of the microstructure evolution of thin films in the presence of grain boundaries and free surfaces. Figure 3 shows simulation results for two systems, which we refer to as thin and thick films. For thin films, the average grain size is similar to the film thickness, while grains in the thick film were ~ 10% the film thickness. Figure 3a depicts the initial configuration, where the lines colored in white denote grain boundary regions. The grey shaded regions at the top and bottom of the films represent the pore space/vacuum. Figure 3b shows the microstructure evolution of both thin and thick films. It can be clearly seen that the thin film developed a columnar structure, where grain boundaries extend perpendicular to the free surfaces. The inset in Figure 3b is a close-up view depicting the surface structure of the thin film, where protrusions of the grains, or the so-called grain

crowning, can be clearly seen. This is in qualitative agreement with the experimental results on pure gold systems, where AFM images show such protrusions [cf. Figure 1b and d].

Future extensions to the modeling framework include: i) accounting for anisotropic grain boundary properties, ii) consideration of alloys and the associated diffusive transport of species, and iii) second phase particles, which act as pinning sites for grain boundary motion.

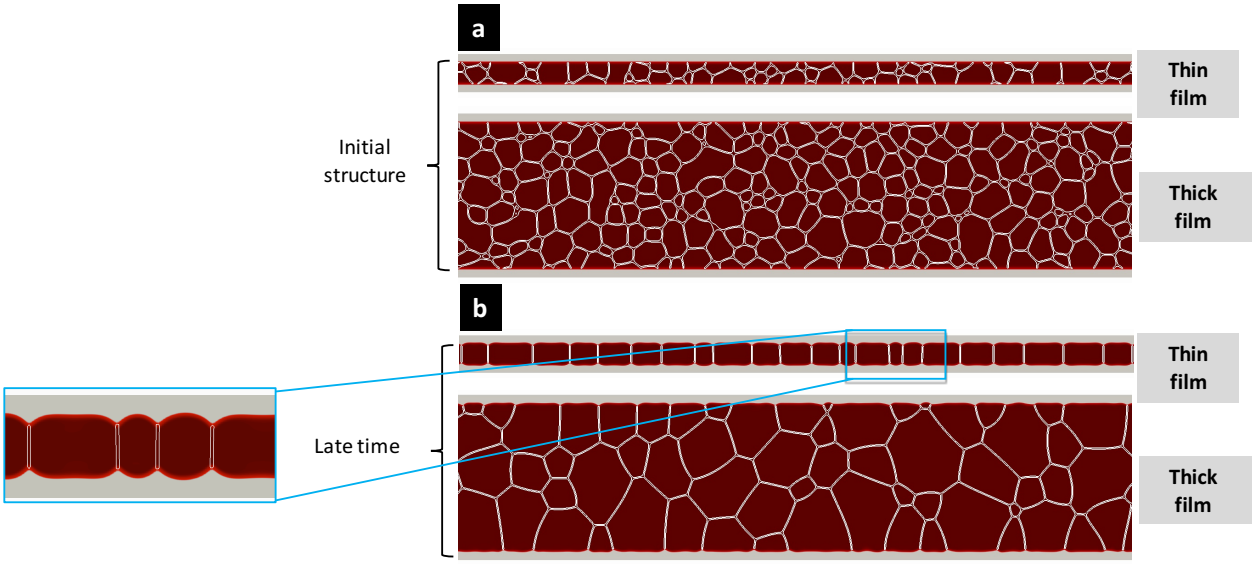

Figure 3: Simulation results of the microstructure evolution of thin and thick films, where (a) depicts the initial state of the films and (b) depicts the final stage. Note the formation of columnar structures in the case of thin films, similar to what is experimentally observed in gold films. The close-up view of the thin film in (b) depicts the protrusion of grains, i.e., grain crowning, when the grooves are spatially close to each other. This effect is experimentally observed, see Figure 1b,d.

Conclusions

The same sample areas smaller than 2 µm × 2 µm in a 40 nm thick nanocrystalline Au foil were characterized before annealing PED and TEM, tracked during stepped annealing to temperatures up to 325 °C *in situ* in the TEM, and characterized further after annealing. This analysis quantified the boundaries between hundreds of grains. Video collected *in situ* during the annealing experiments allowed for the quantification of grain boundary migration velocities of the same grains that had been characterized structurally. Additional characterization of the film surfaces was performed by AFM before and after the anneals, revealing the formation of distinct plate-like surface structures.

Acknowledgments

The experimental work was conducted by Daniel Bufford and Khalid Hattar. Development of the phase field model and simulation results was done by Fadi Abdeljawad. The author(s) acknowledge D.P. Adams, A. Baca, C. Sobczak (Sandia National Laboratories).

References

[1] D. A. Porter and K. E. Easterling, Phase Transformations in Metals and Alloys, 2 ed. New York: Chapman and Hall, 1992.

[2] E. R. Homer, S. M. Foiles, E. A. Holm, and D. L. Olmsted, "Phenomenology of shear-coupled grain boundary motion in symmetric tilt and general grain boundaries," Acta Materialia, vol. 61, pp. 1048-1060, Feb 2013.

[3] V. Y. Aristov, V. Y. Fradkov, and L. S. Shvindlerman, "Interaction of Moving Grain-Boundary with Crystal-Surface," Fizika Metallov I Metallovedenie, vol. 45, pp. 997-1008, 1978.

[4] E. F. Rauch, J. Portillo, S. Nicolopoulos, D. Bultreys, S. Rouvimov, and P. Moeck, "Automated nanocrystal orientation and phase mapping in the transmission electron microscope on the basis of precession electron diffraction," Zeitschrift Fur Kristallographie, vol. 225, pp. 103-109, 2010.

[5] K. Hattar, D. Bufford, and D. L. Buller, "Concurrent In situ Ion Irradiation Transmission Electron Microscope," Nuclear Instruments & Methods in Physics Research Section B-Beam Interactions with Materials and Atoms, vol. 338, pp. 56-65, 2014.

Acronym/Abbreviation List

AFM	Atomic force microscopy
TEM	Trasmission electron microscopy
PED	Precession Electron Diffraction